

**Original Research Article****Composition dependent structural and optical properties of nanocrystallites  $\text{Zn}_x\text{Cd}_{1-x}\text{S}$** **ABSTRACT**

In this work a novel chemical reduction method at room temperature is described to synthesize nanocrystalline  $\text{ZnS}$ ,  $\text{CdS}$ ,  $\text{Zn}_x\text{Cd}_{1-x}\text{S}$ . The method is cheap and cost effective. The grown nanoparticles are characterized by XRD, TEM, EDX, UV-VIS absorption and PL study.  $\text{CdS}$  formation is supported by the systematic splitting of x-ray diffraction peak at lower angle and the peaks are identified.  $\text{ZnS}$  peaks are also identified comparing with ICDD data. EDX analysis shows two other phases  $\text{Zn}_{0.8}\text{Cd}_{0.2}\text{S}$ ,  $\text{Zn}_{0.5}\text{Cd}_{0.5}\text{S}$ . The particle sizes are in the range 4-8 nm. The band gap changes with change of composition. Also at each composition the band gap is greater compared to bulk band gap. This indicates quantum confinement takes place. The band gap energy of nanoparticles can be tuned to a lower energy by increasing the Cd content, indicating the formation of the alloyed nanoparticles. PL peak shifts towards higher wavelength as Cd content increases. The peak corresponds to transition associated with surface state.

**Keywords:**  $\text{Zn}_x\text{Cd}_{1-x}\text{S}$  nanoparticles , structural properties, Optical properties, Photoluminescence

**1. INTRODUCTION**

The synthesis and characterization of semiconductor nanoparticles have attracted much interest because of their novel properties as a consequence of the large number of surface atoms and the three-dimensional confinement of the electrons [1-7]. Altering the size of the particles alters the degree of the confinement of the electrons and affects the electronic structure of the solid, especially the band gap edges.

Among a variety of semiconductor materials, the binary metal chalcogenides of group II-VI have been extensively studied [1-16]. For example, nanocrystalline thin films of  $\text{ZnS}$  and  $\text{CdS}$  are attractive materials in photoconducting cells and optoelectronic devices such as solar cells and photodetectors [17-19].

Alloying of semiconductors is one of the simplest techniques used for tailoring the energy band gap, lattice parameter, electronic and optical properties[20] Generally in alloys, the lattice parameter varies linearly with composition and follows the Vegard's law.

Among the different ternary II-VI semi-conductors,  $\text{Zn}_x\text{Cd}_{1-x}\text{S}$  has been widely used as a wide band gap material in heterojunction solar cells[21–23] , photoconductive devices[24],high-density optical recording and for blue or even ultraviolet laser diodes [25-29].

In this paper, we report a novel chemical reduction route to  $\text{ZnS}$ ,  $\text{CdS}$  and  $\text{Zn}_x\text{Cd}_{1-x}\text{S}$  nanocrystals at room temperature

**2. EXPERIMENTAL SECTION**

Typically, an appropriate amount of sulfur powder was added to a flask containing 50 mL of tetrahydrofuran (THF). After being stirred magnetically for 5 min, the mixture became a colorless transparent solution. A stoichiometric amount of  $\text{ZnCl}_2$  was added to the flask and a black suspension formed upon stirring. After the addition of  $\text{NaBH}_4$ , the suspension turned light green. After the mixture was stirred for 10h, a white precipitate formed. Then the precipitate was centrifuged and dried at room temperature. The sample is now ready for characterization. For the preparation of nanocrystalline  $\text{CdS}$ , the process was the same as above except that anhydrous  $\text{CdCl}_2$  was used instead of  $\text{ZnCl}_2$ .

For the preparation of  $\text{Zn}_x\text{Cd}_{1-x}\text{S}$  stoichiometric anhydrous  $\text{ZnCl}_2$  and  $\text{CdCl}_2$  powders were used according to the molar ratios in the target compounds  $\text{Zn}_{0.7}\text{Cd}_{0.3}\text{S}$ ,  $\text{Zn}_{0.5}\text{Cd}_{0.5}\text{S}$ . The X-ray powder diffraction (XRD) was obtained using a Rigaku MiniFlex-II X-ray Diffractometer using  $\text{CuK}_\alpha$  radiation. Transmission electron microscope (TEM) images were obtained using the JEOL JEM-200 TEM operated at 200 kV. UV-VIS absorption spectra were recorded using a Shimadzu Pharmaspec-1700 spectrophotometer with a 1-cm quartz cell at room temperature. Colloid solutions in ethanol were prepared ultrasonically for the UV-VIS and the photoluminescence (PL) measurements. The Photoluminescence of  $\text{ZnS}$ ,  $\text{CdS}$  and  $\text{Zn}_x\text{Cd}_{1-x}\text{S}$  nanoparticles were measured using Perkin Elmer LS 55 Fluorescence Spectrometer.

### 3. RESULTS AND DISCUSSION

Fig. 1 shows the x-ray diffraction peaks of the as prepared  $\text{ZnS}$ ,  $\text{CdS}$  and different  $\text{Zn}_x\text{Cd}_{1-x}\text{S}$  samples. Samples are taken in the powder form and the measured angle is within 20-60 degree. Results show well defined peaks in each case and the peak positions gradually change with composition of the samples. All XRD patterns show obvious size broadening effect. In case of  $\text{CdS}$  the half width of the first peak is maximum indicating that particle size is minimum which is also confirmed by TEM pattern. For  $\text{CdS}$  the XRD pattern can be indexed as a wurtzite phase structure with strongly characteristic (100), (002), (101), (102), (110), (103) and (112) peaks, while for  $\text{ZnS}$  XRD pattern mainly reflects its zincblende character [(111), (220) and (311) peaks] with some wurtzite character [such as the existence of a vague (103)], which indicates either that the  $\text{ZnS}$  particles have a zincblende structure with some wurtzite stacking faults or that most particles have a zincblende structure with others having a wurtzite structure. As for the  $\text{Zn}_x\text{Cd}_{1-x}\text{S}$  nanocrystals the diffraction peaks in the XRD patterns gradually shift to larger angles and a phase transition from wurtzite to zincblende occurs with an increase of  $\text{Zn}$  content. This continuous peak shifting of the nanocrystals also indicates that there is no phase separation or separated nucleation of  $\text{ZnS}$  or  $\text{CdS}$  in the  $\text{Zn}_x\text{Cd}_{1-x}\text{S}$  nanocrystals.

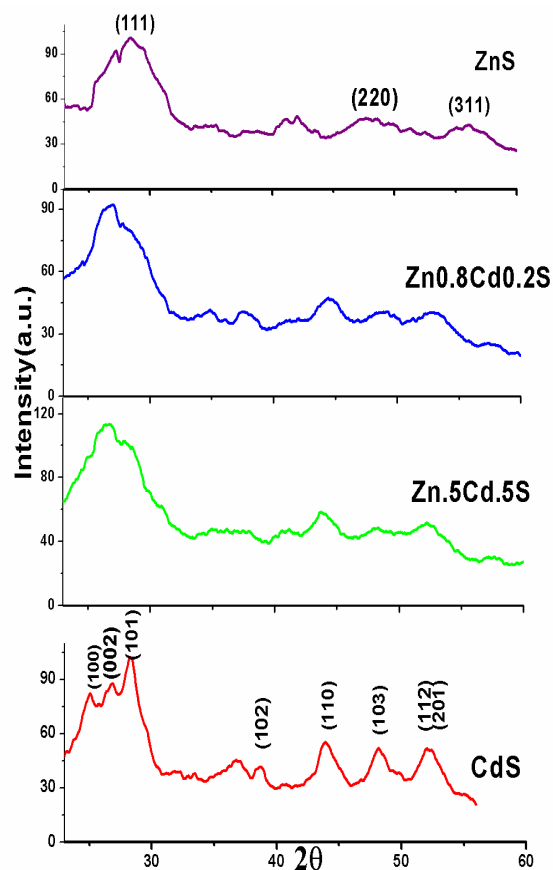
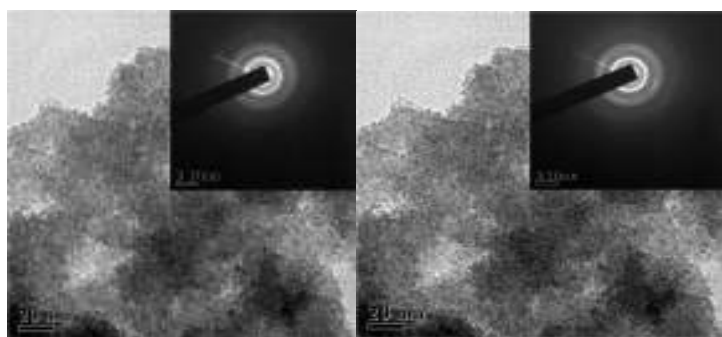


Figure.-1 The XRD pattern of the as prepared samples.

68

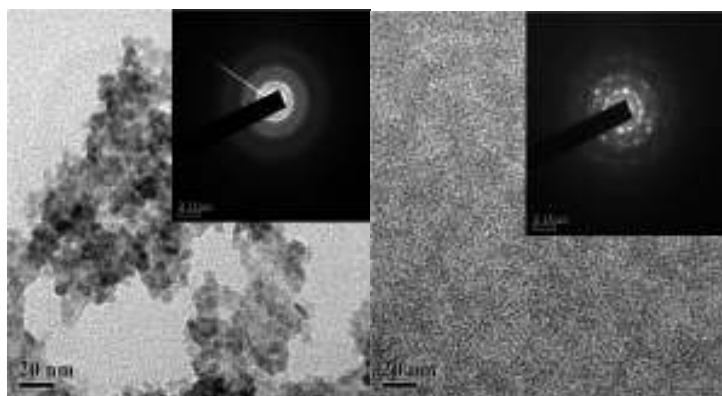


69

70 Fig. 2(a)

Fig. 2(b)

71



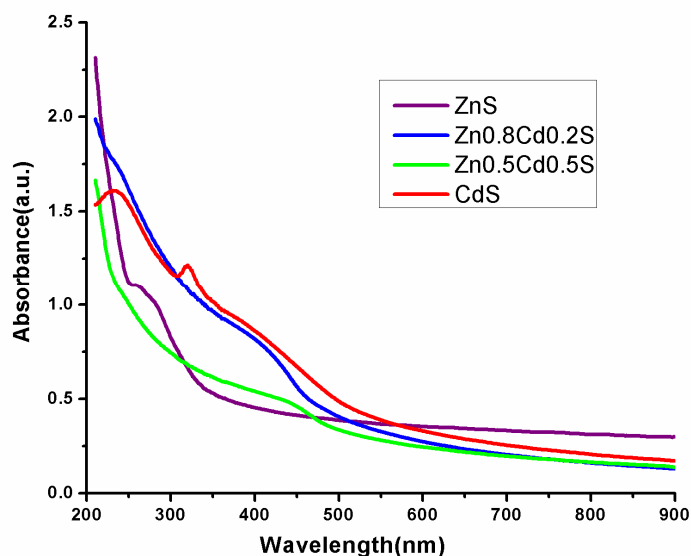
72

73 Fig. 2(c)

Fig. 2(d)

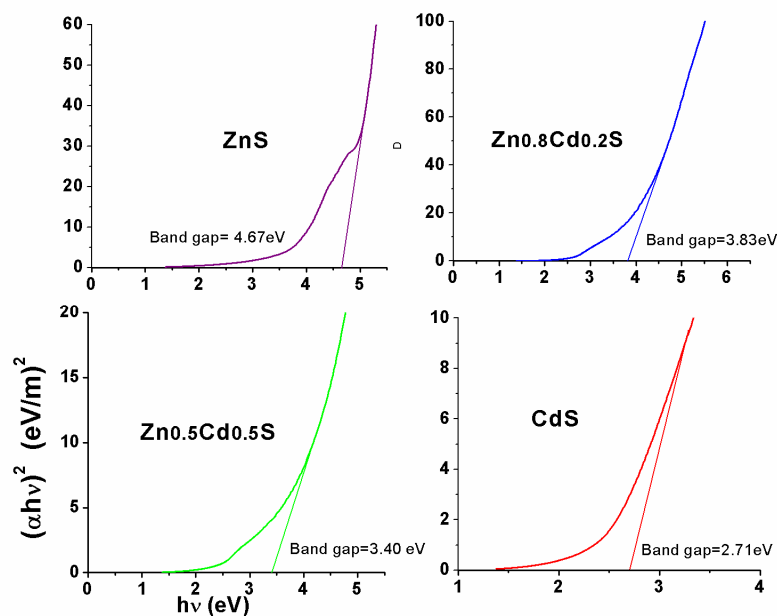
74 Figure :-2 The TEM pattern of as synthesized (a) ZnS (b)  $\text{Zn}_{0.8}\text{Cd}_{0.2}\text{S}$  (c)  $\text{Zn}_{0.5}\text{Cd}_{0.5}\text{S}$  (d) CdS  
 75 Samples are well dispersed in ethanol by ultrasonification and it is placed on the carbon coated grid  
 76 for TEM measurement. Fig.2 (a, b, c, d) shows TEM pattern of the as prepared samples. The particle  
 77 size is measured in each case from the photograph.

78 TEM analysis indicates that the particles are in the nano range for different samples. Particle size for  
 79 ZnS is found to be 4 nm. Particle size gradually increases with increase of Cd content. But in case of  
 80 CdS particle size is reduced. Also from TED pattern it is observed that in case of CdS diffraction dots  
 81 predominates ring. Hence CdS nanoparticles show single crystallinity. Other three phases show  
 82 polycrystalline nature. EDX analysis show the composition of the obtained material. There is difference  
 83 of the target material and the obtained material for the composition  $\text{Zn}_{0.8}\text{Cd}_{0.2}\text{S}$ .



84

85 Figure.-3 Optical absorption spectra of different samples.



86

87 Figure.-4 The band gap determination curve for different samples.

88

89 Optical absorption of the dispersed samples are taken using a spectrophotometer and the data is  
 90 recorded in the range of 200-900 nm. Fig.3 displays the absorption spectra of the different samples.  
 91 Optical absorption coefficient ( $\alpha$ ) is calculated at each wave length. The band gaps of the as-prepared  
 92 nanoparticles are determined from the relation

$$93 \quad (\alpha h\nu)^2 = C(h\nu - E_g)$$

94 Where  $C$  is a constant.  $E_g$  is the band gap of the material and  $\alpha$  is the absorption coefficient.

95 Fig. 4 shows the plot of  $(\alpha h\nu)^2$  vs. energy ( $h\nu$ ) and it is used to determine band gap in each case.

From the optical absorption study it is found that band gap decreases with increase of Cd content. The decrease of band gap is attributed to the increase of particle size as well as the stoichiometric variation of Cd with respect to Zn. But in each sample band gap is found to be greater than the bulk band gap. This clearly indicates quantum confinement takes place in each sample.

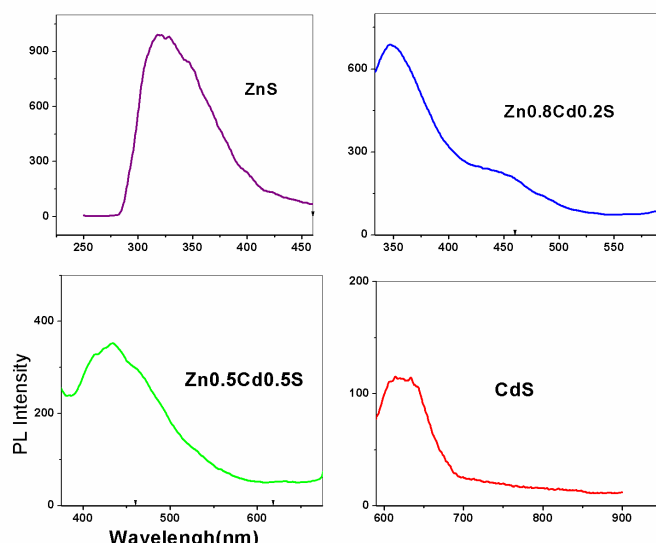


Figure-5 The photoluminescence spectra of as synthesized samples.

Fig .5 displays the PL spectra of the samples dispersed in ethanol.PL peaks are shifted to higher wavelength as Cd content increases.

**Table 1. Summarisation Table**

Target Material	Obtained Material	PL PEAK(nm)	PARTICLE SIZE(nm)	BAND GAP (eV)
ZnS	ZnS	320	4	4.67
Zn <sub>0.7</sub> Cd <sub>0.3</sub> S	Zn <sub>0.8</sub> Cd <sub>0.2</sub> S	348	5.4	3.83
Zn <sub>0.5</sub> Cd <sub>0.5</sub> S	Zn <sub>0.5</sub> Cd <sub>0.5</sub> S	435	8.0	3.40
CdS	CdS	621	4.5	2.71

## 4. CONCLUSION

[The above results reveal that ZnS, CdS and Zn<sub>x</sub> Cd<sub>1-x</sub> S nanoparticles are successfully obtained at room temperature and the compositions have been controlled. It is observed that by changing the ratio of ZnCl<sub>2</sub>, CdCl<sub>2</sub> in the reactants the two phases Zn<sub>0.8</sub> Cd<sub>0.2</sub> S and Zn<sub>0.5</sub> Cd<sub>0.5</sub> S are obtained.The control of the composition of Zn<sub>x</sub> Cd<sub>1-x</sub> S nanoparticles may lead to the development of ideal materials for short wavelength diode laser applications.

## REFERENCES

- [1] Henglein, A.: Small-particle research: physicochemical properties of extremely small colloidal metal and semiconductor particles. Chemical Reviews. 1989;89(8):1861-1873.
- [2] Steigerwald, M. L., & Brus, L. E.: Semiconductor crystallites: a class of large molecules. Accounts of Chemical Research. 1990;23(6):183-188.

- 125 [3] Bawendi, M. G., Steigerwald, M. L., & Brus, L. E.: The quantum mechanics of larger  
126 semiconductor clusters ("quantum dots"). Annual Review of Physical Chemistry. 1990;41(1):477-  
127 496.
- 128 [4] Wang, Y., & Herron, N.: Nanometer-sized semiconductor clusters: materials synthesis, quantum  
129 size effects, and photophysical properties. The Journal of Physical Chemistry. 1991;95(2):525-  
130 532.
- 131 [5] Weller, H. :Quantized semiconductor particles: a novel state of matter for materials  
132 science. Advanced Materials.1993;5(2):88-95.
- 133 [6] Alivisatos, A. P. :Semiconductor clusters, nanocrystals, and quantum dots. Science.  
134 1996; 271(5251): 933.
- 135 [7] Eychmüller, A. :Structure and photophysics of semiconductor nanocrystals. The Journal of  
136 Physical Chemistry B. 2000;104(28):6514-6528.
- 137 [8] Bawendi, M. G., Wilson, W. L., Rothberg, L., Carroll, P. J., Jedju, T. M., Steigerwald, M. L., &  
138 Brus, L. E. Electronic structure and photoexcited-carrier dynamics in nanometer-size CdSe  
139 clusters. Physical Review Letters. 1990;65(13):1623.
- 140 [9] Rossetti, R., Hill, R., Gibson, J. M., Brus, L. E.: Excited electronic states and optical spectra of ZnS  
141 and CdS crystallites in the  $\approx 15$  to 50 Å size range: evolution from molecular to bulk  
142 semiconducting properties. The Journal of chemical physics. 1985;82 (1): 552-559.
- 143 [10] Weller, H. :Colloidal semiconductor Q-particles: chemistry in the transition region between solid  
144 state and molecules. Angewandte Chemie International Edition in English. 1993;32(1): 41-53.
- 145 [11] Mann, S.: Molecular recognition in biomineralization. Nature. 1988;332,119–124.  
146 doi:10.1038/332119a0
- 147 [12] Braun, P. V., Osenar, P., & Stupp, S. I. : Semiconducting superlattices templated by molecular  
148 assemblies. Nature. 1996;380(6572):325-328.
- 149 [13] Greenham, N. C., Peng, X., & Alivisatos, A. P. :Charge separation and transport in conjugated-  
150 polymer/semiconductor-nanocrystal composites studied by photoluminescence quenching and  
151 photoconductivity. Physical review B. 1996; 54(24):17628.
- 152 [14] Dinsmore, A. D., Hsu, D. S., Gray, H. F., Qadri, S. B., Tian, Y., & Ratna, B. R. :Mn-doped ZnS  
153 nanoparticles as efficient low-voltage cathodoluminescent phosphors. Applied physics letters.  
154 1999;75(6):802-804.
- 155 [15] Maity, R., & Chattopadhyay, K. K. :Synthesis and optical characterization of ZnS and ZnS: Mn  
156 nanocrystalline thin films by chemical route. Nanotechnology. 2004;15(7):812.
- 157 [16] Deng, Z., Qi, J., Zhang, Y., Liao, Q., & Huang, Y.: Growth mechanism and optical properties of  
158 ZnS nanotetrapods. Nanotechnology. 2007;18(47):475603.
- 159 [17] Oladeji, I. O., & Chow, L. :Synthesis and processing of CdS/ZnS multilayer films for solar cell  
160 application. Thin Solid Films. 2005;474(1):77-83.
- 161 [18] Wang, X., Xie, Z., Huang, H., Liu, Z., Chen, D., & Shen, G.: Gas sensors, thermistor and  
162 photodetector based on ZnS nanowires. Journal of Materials Chemistry, 2012;22(14):6845-6850.
- 163 [19] Liang, Y., Liang, H., Xiao, X., & Hark, S.: The epitaxial growth of ZnS nanowire arrays and their  
164 applications in UV-light detection. Journal of Materials Chemistry, 2012; 22(3): 1199-1205.
- 165 [20] Romeo, N., Sberveglieri, G., & Tarricone, L. :Low-resistivity ZnCdS films for use as windows in  
166 heterojunction solar cells. Applied Physics Letters.1978;32(12):807-809.
- 167 [21] Reddy, K. R., & Reddy, P. J. :Studies of  $\text{Zn}_x\text{Cd}_{1-x}\text{S}$  films and  $\text{Zn}_x\text{Cd}_{1-x}\text{S}/\text{CuGaSe}_2$   
168 heterojunction solar cells. Journal of Physics D: Applied Physics.1992;25(9):1345.
- 169 [22] Mitchell, K. W., Fahrenbruch, A. L., & Bube, R. H. : Evaluation of the CdS/CdTe heterojunction  
170 solar cell. Journal of Applied Physics, 1977;48(10):4365-4371.
- 171 [23] Basol, B. M. : High-efficiency electroplated heterojunction solar cell. Journal of Applied Physics,  
172 1984;55(2):601-603.
- 173 [24] Torres, J., & Gordillo, G. :Photoconductors based on  $\text{Zn}_x\text{Cd}_{1-x}\text{S}$  thin films. Thin Solid Films,  
174 1992;207(1):231-235.
- 175 [25] WU BJ; Cheng H; Guha S; Haase MA; Depuydt JM; Meishaugen G; Qiu J.: Molecular-beam  
176 epitaxial-growth of cdzns using elemental sources. Applied physics letters, 1993;63(21):2935-  
177 2937.

- 178 [26] Guha, S., Wu, B. J., Cheng, H., & DePuydt, J. M. :Microstructure and pseudomorphism in  
179 molecular beam epitaxially grown ZnCdS on GaAs (001).Applied physics  
180 letters, 1993;63(15):2129-2131.
- 181 [27] Haase, M. A., Qiu, J., DePuydt, J. M., & Cheng, H. ;Blue-green laser diodes. Applied Physics  
182 Letters, 1991;59(11):1272-1274.
- 183 [28] Jeon, H., Ding, J., Patterson, W., Nurmikko, A. V., Xie, W., Grillo, D. C., ... & Gunshor, R. L.  
184 :Blue-green injection laser diodes in (Zn, Cd) Se/ZnSe quantum wells. Applied physics letters,  
185 1991;59(27):3619-3621.
- 186 [29] Yamaga, S., & Yoshikawa, A. :Dependence of electrical and optical properties of iodine-doped  
187 cubic ZnCdS films on solid composition. Journal of crystal growth, 1992;117(1):353-357.